Study of the quenched lifetime of an interacting positronium gas

2014 J. Phys. B: At. Mol. Opt. Phys. 47 155202

(http://iopscience.iop.org/0953-4075/47/15/155202)

IOP Publishing Journal of Physics B: Atomic, Molecular and Optical Physics

J. Phys. B: At. Mol. Opt. Phys. **47** (2014) 155202 (9pp) doi:10.1088/0953-4075/47/15/155202

Study of the quenched lifetime of an interacting positronium gas

O Morandi, P-A Hervieux and G Manfredi

Institut de Physique et Chimie des Matériaux de Strasbourg, CNRS and University of Strasbourg 23, rue du Loess, F-67034 Strasbourg, France

E-mail: omar.morandi@ipcms.unistra.fr

Received 31 January 2014, revised 10 June 2014
Accepted for publication 13 June 2014
Published 28 July 2014

Abstract

By using a kinetic approach, we study the evolution of a gas composed of interacting ortho- and para-positronium atoms. We calculate the total lifetime of the gas and study the ortho-positronium quenching effect induced by the bi-atomic scattering mechanisms with spin exchange. We analyze a realistic situation where the positronium is formed by highly energetic positrons impinging on a solid surface. In the case of a spin-polarized source of positrons, the spinpolarization time of the final positronium gas is estimated.

Keywords: positronium dynamics, quenching of positronium, positronium binary-collisions, boltzmann dynamics, gas thermalization dynamics

(Some figures may appear in colour only in the online journal)

1. Introduction

The positron is the most easily produced kind of antiparticle. At low density and temperature, positrons and electrons can form a bound state known as positronium (Ps). The ground state of the positronium consists of triplet states with total spin one (ortho-positronium ^{3}Ps) and a singlet state with total spin zero (para-positronium ^{1}Ps) separated by a hyperfine energy gap [1]. The ortho-positronium and para-positronium states are represented as follows

$$\left.\begin{aligned} |1,1\rangle &= |e^-\uparrow, e^+\uparrow\rangle \\ |1,0\rangle &= \frac{1}{\sqrt{2}}\left(|e^-\uparrow, e^+\downarrow\rangle + |e^-\downarrow, e^+\uparrow\rangle\right) \\ |1,-1\rangle &= |e^-\downarrow, e^+\downarrow\rangle \end{aligned}\right\} : {}^3\mathrm{Ps} \qquad (1)$$

$$\left.\begin{aligned} |0,0\rangle &= \frac{1}{\sqrt{2}}\left(|e^-\uparrow, e^+\downarrow\rangle - |e^-\downarrow, e^+\uparrow\rangle\right) \end{aligned}\right\} : {}^1\mathrm{Ps} \qquad (2)$$

On the left-hand side, the two-particle state is described by the angular momentum of the atom $|S, m\rangle$, where $S = 0,1$ is total angular momentum and $m = -S, 0, S$ is the spin projection along the direction of quantization. On the right-hand side, we indicate the spin components of the two particles that compose the positronium (e^- denotes the electron and e^+ the positron). The total angular momentum of the positronium determines the lifetime and the decay channels of the atom. Ortho-positronium has a lifetime of 142 ns and annihilates into three photons, while para-positronium annihilates in 125 ps by emitting two gamma photons. Ortho-positronium can be quickly turned into para-positronium by using an oscillating magnetic field [2].

Advanced experiments, such as the production of a positronium Bose–Einstein condensate [3] and the measurement of the gravitational acceleration on antimatter [4], may be feasible provided that a dense gas of positronium atoms is cooled at cryogenic temperature and confined into nanometric cavities or diffused in a vacuum.

Moreover, the creation of a long-lived confined Ps gas has a direct application to the production of the antihydrogen ($\overline{\mathrm{H}}$) atom [5]. Antihydrogen atoms have been already produced by some international collaborations [6, 7]. The method employed consisted of trapping together positrons and antiprotons. Alternatively, cold antihydrogen atoms can be obtained by the charge exchange reaction $\overline{p} + {}^3\mathrm{Ps}^* \rightarrow \overline{\mathrm{H}} + e^-$, where $\overline{p}$ denotes the antiproton and the star indicates an excited ^{3}Ps state (Rydberg positronium) [8].

One of the most developed techniques for the production of trapped and free Ps (either in the ground or in an excited state [9]) consists of implanting positrons with energies of a few keV in a porous material (typically silica) [10]. At the

distance of roughly 100 nm from the external surface of the material, the particle motion becomes diffusive and the positrons are likely to capture an electron from the solid and form an atom of positronium. The positronium atoms are easily trapped inside solids that contain pores or cavities. The gas that is formed is made of a statistical mixture of ortho- and para-positronium atoms. The lifetime of the positronium produced in the solid can be probed by detecting the gamma-ray radiation produced by the electron-positron annihilation. In such a way, it is possible to measure the density of the different atomic species that compose the gas. Typically, such a spectrum contains several exponentially decaying components: a short-lived component (particle lifetime inferior to 1 ns) due to para-positronium and free positrons, a component due to o–Ps annihilating in the bulk (lifetime of a few ns), and a long-lived component produced by the o–Ps annihilation in the pore (lifetime up to 140 ns). The measurement of the positronium lifetime in a cavity has been performed in [11]. In [12], a Monte Carlo method is employed for the estimation of the lifetime of a single positronium atom trapped in a spherical cavity.

The technique of positron implantation in materials containing cavities or defects for the production of free positronium dates back to the seventies, when Brandt and Paulin observed the diffusion in free space of the ortho-positronium formed in fine oxide powders [13]. Similar experiments proved that in various porous and mesoporous materials, such as silica aerogels and porous glasses, a significant fraction of ortho-positronium formed inside the material is trapped in the pores (see e. g. [14, 15] and, for more recent achievements [16–20]). In such materials, the size of the pores spans from a few to hundreds of nanometers. In particular, porous silica and silica aerogels are particularly efficient for the formation of positronium (more than 50% of implanted positrons are able to capture one electron of the silica and form a positronium atom) [21]. Films of porous silica have been employed for the creation of excited atomic states, the di-positronium molecule [22], and the detection of the quenched lifetime [22, 24, 25]. After the injection, the positronium gas is cooled by the collisions of the atoms with the pore surface and, in the presence of interconnected porosities, the gas may escape into the vacuum [10, 26].

Positronium quenching effect. The injection of an intense positron pulse into a porous material could lead to the creation of a high density gas of confined positronium atoms that interact with each other [24]. One of the major challenges in the experimental study of positronium is the necessity to perform all the operations within the short lifetime of this metastable atom. In positronium gases that are sufficiently dense, the Ps–Ps interaction could cause an additional decrease of the total lifetime of the gas. In particular, various interaction channels cause the conversion of long-lived triplet atoms into singlet states that are quickly removed from the system. The reduction of the ortho-positronium lifetime due to the creation of short-lived states by bi-atomic collisions is denoted as the positronium quenching mechanism.

According to equations (1)–(2), the low energy positronium states are characterized by the relative spin configuration of the positron and the electron. Consequently, by controlling the spin polarization of the particles, it is possible to modify the densities of the positronium populations (we have three possible states in the o–Ps configuration and one p–Ps state). One practical advantage of using a spin-polarized positronium gas is that, when the gas is fully polarized, all the atomic conversion processes are suppressed. In this case, the only remaining interaction channel is the bi-atomic hard sphere collision. As a consequence, the ortho-positronium lifetime is no longer limited by the quenching processes. However, in the experiments where the positronium is created via the implantation of positrons, the positrons are usually unpolarized. In this case, the four lowest energy levels of the positronium, the singlet and the three triplet states, are created with equal probability. As an alternative, a spin-polarized gas of positronium can be created by employing some radioactive materials (typically sodium) that are a natural source of high-energy spin-polarized positrons. The polarization of the positrons can be maintained during the entire process of positronium formation. However, also in this case, the initial spin polarization of the positronium gas cannot exceed 30%. Once a statistical mixture of spin-up and spin-down atoms of positronium is formed, several reactions start to modify the composition of the gas. The most important process is the suppression by annihilation of the minority spin atoms with the same amount of atoms with opposite spin. As a result, the gas becomes fully spin-polarized.

By using this technique, Cassidy *et al* were able to produce a fully polarized gas of orthopositronium in a porous material [27]. Specifically, a highly spin-polarized ortho-positronium gas (96%) was formed in a silica pore less than 50 ns after implantation.

In this contribution, we simulate the modification of the chemical composition of a gas containing a mixture of singlet and triplet populations, due to the bi-atomic collision processes. The Ps gas dynamics is modeled by using the Boltzmann approach, which is particularly adapted to the description of chemical reactions in interacting particle systems.

The paper is organized as follows. In section 2 we present the mathematical model that we use for the simulation of a gas of interacting positronium atoms. We include all the relevant chemical reactions that convert one positronium population into another, with consequent modification of the total lifetime of the gas. Some details concerning our numerical discretization method are discussed. The results of our simulations are presented in section 3. In order to analyze the spin quenching effects, we consider different positronium gases, where the initial density and polarization are varied. In section 4 we draw our conclusions.

2. Ps–Ps interaction: mathematical model

In this section, we study the spin polarization of a gas of interacting positronium atoms. In particular, we focus on the quenching of the positronium (γ-annihilation) enhanced by the Ps–Ps mutual spin conversion.

We consider the evolution of a gas constituted by a mixture of triplet and singlet positronium states. The particle

Table 1. Bi-atomic collision processes included in our model. The left column describes the two-body chemical reactions in terms of the incoming and outcoming atomic configurations. The cross sections are given in the middle column, and in the right column we indicate their numerical value (taken from [37]). $A_0 = 0.44$ nm and $A_1 = 0.15$ nm.

Chem. Reaction	Cross section	Numerical value
	o–Ps ↔ o–Ps	
$\|1,0\rangle \cdot \|1,1\rangle \rightarrow \|1,0\rangle \cdot \|1,1\rangle$	$\sigma_{10,11\rightarrow 10,11} = \sigma_{10,1-1\rightarrow 10,1-1}$	$8\pi A_1^2$
$\|1,0\rangle \cdot \|1,0\rangle \rightarrow \|1,0\rangle \cdot \|1,0\rangle$	$\sigma_{10,10\rightarrow 10,10}$	$2\pi(\frac{A_0}{2} + \frac{3A_1}{2})^2$
$\|1,0\rangle \cdot \|1,0\rangle \rightarrow \|1,1\rangle \cdot \|1,-1\rangle$	$\sigma_{10,10\rightarrow 11,1-1} = \sigma_{11,1-1\rightarrow 10,10}$	$\pi(A_0 - A_1)^2$
$\|1,1\rangle \cdot \|1,-1\rangle \rightarrow \|1,1\rangle \cdot \|1,-1\rangle$	$\sigma_{11,1-1\rightarrow 11,1-1}$	$2\pi(A_0 + A_1)^2$
$\|1,1\rangle \cdot \|1,1\rangle \rightarrow \|1,1\rangle \cdot \|1,1\rangle$	$\sigma_{11,11\rightarrow 11,11} = \sigma_{1-1,1-1\rightarrow 1-1,1-1}$	$8\pi A_1^2$
	o–Ps ↔ p–Ps	
$\|1,0\rangle \cdot \|1,0\rangle \rightarrow \|0,0\rangle \cdot \|0,0\rangle$	$\sigma_{10,10\rightarrow 00,00}$	$\pi\frac{1}{2}(A_0 - A_1)^2$
$\|1,1\rangle \cdot \|1,-1\rangle \rightarrow \|0,0\rangle \cdot \|0,0\rangle$	$\sigma_{11,1-1\rightarrow 00,00}$	$\pi(A_0 - A_1)^2$
	p–Ps ↔ p–Ps	
$\|0,0\rangle \cdot \|0,0\rangle \rightarrow \|0,0\rangle \cdot \|0,0\rangle$	$\sigma_{00,00\rightarrow 00,00}$	$\frac{1}{2}\pi(A_0 + 3A_1)^2$
	o–Ps,p–Ps ↔ o–Ps,p–Ps	
$\|0,0\rangle \cdot \|1,0\rangle \rightarrow \|0,0\rangle \cdot \|1,0\rangle$	$\sigma_{00,10\rightarrow 00,10}$	$4\pi A_1^2$
$\|0,0\rangle \cdot \|1,1\rangle \rightarrow \|0,0\rangle \cdot \|1,1\rangle$	$\sigma_{00,11\rightarrow 00,11} = \sigma_{00,1-1\rightarrow 00,1-1}$	$4\pi A_1^2$

dynamics is treated at the classical level. The various populations of positronium are described by a set of classical distribution functions denoted by $f_{1,1}$ $f_{1,0}$ $f_{1,-1}$ for the ortho-positronium, and $f_{0,0}$ for the para-positronium.

The atomic collision processes, with consequent modification of the spin configuration, are described by a kinetic approach. Kinetic models based on the Boltzmann equation have been used by various authors for the description of the evolution of boson gases in various regimes [28–30]. In the kinetic formalism, the evolution of the *i*th Ps population of the gas f_i is given by the Boltzmann equation

$$\frac{\partial f_i}{\partial t} = c\sum_{j,r,s}\int\Big[\Big(1+f_i(\mathbf{p})\Big)\Big(1+f_j(\mathbf{p}_1)\Big)f_r(\mathbf{p}_2)f_s(\mathbf{p}_3) - f_i(\mathbf{p})f_j(\mathbf{p}_1)\Big(1+f_r(\mathbf{p}_2)\Big)\Big(1+f_s(\mathbf{p}_3)\Big)\Big] \times\sigma_{i,j\rightarrow r,s}\delta\Big[E(\mathbf{p})+E(\mathbf{p}_1)-E(\mathbf{p}_2) - E(\mathbf{p}_3)\Big]\delta\Big(\mathbf{p}+\mathbf{p}_1-\mathbf{p}_2-\mathbf{p}_3\Big)\,\mathrm{d}\mathbf{p}_1\,\mathrm{d}\mathbf{p}_2\,\mathrm{d}\mathbf{p}_3 - \frac{f_i}{\tau_i}. \quad (3)$$

Here, $c = \frac{2}{\pi\hbar^3 m^3}$, τ_1 is the lifetime if the *i*-th population, m denotes the mass of the positronium and $E(\mathbf{p}) = \frac{\mathbf{p}^2}{2m}$. The balance equation (3) describes the bi-atomic scattering processes where two atoms (*i* and *j* in the formula) undergo a short-range, hard-sphere collision. As a result, the atoms *r* and *s* are generated. The factors $1 + f$ in the formula take into account the bosonic nature of the positronium. Finally, the presence in the integral of the two Dirac delta distributions ensures the conservation of the total energy and momentum during each scattering event. The scattering cross section $\sigma_{i,j\rightarrow r,s}$ gives the strength of the interaction. The theoretical study of the low-energy diffusion processes of two Ps atoms has been performed by various authors [31–34]. In our code, we include all the relevant two-body Ps–Ps interactions, which are listed in table 1 (a clear synthesis of these processes can be found in [35]). Here, we refer to the calculations performed by Ivanov *et al* [36]. In particular, we used the following values for the scattering lengths $A_0 = 8.44\ a_0 = 0.44$ nm, $A_1 = 3\ a_0 = 0.15$ nm, where $a_0 = 5.29 \times 10^{-2}$ nm is the Bohr radius. We distinguish two type of reactions. The scattering processes with atomic conversion (where an atom of o–Ps is converted into an atom of p–Ps or vice versa) and processes without atomic conversion. In particular, the reactions that belong to the second group do not change the lifetime of the positronium.

In our model, we do not include the reactions that lead to the formation of the di-positronium molecule Ps_2. The creation of the Ps_2 is a three-body process. It was proved by Cassidy and Mills that it is possible to produce Ps_2 by the simple diffusion of positrons inside a porus silica sample [22, 23]. They gave strong evidence that, rather than by the collisions among three positronium atoms, the Ps_2 molecule is formed by two-body collisions in the presence of a surface state that plays the role of the third body (so that the conservation of the total momentum can be fulfilled). The experiments showed that the Ps_2 molecule is produced only in the proximity of the pore surface. For this reason, until today the di-positronium molecule was only observed in porous materials containing small (≈ 4 nm) disordered pores. The reason should be ascribed to the competition between the processes that lead to the molecule formation and all the other processes, characterized by spin exchange, that lead to the quenching of the positronium. In a large pore, the 'normal'

spin-exchange quenching processes are dominant (we call 'normal' processes all the scattering mechanisms described in table 1). Consequently, the positronium population with minority spin is rapidly quenched before the production of Ps_2 can become significant. In the case of small pores, the normal quenching mechanisms are suppressed and the di-positronium molecule can thus be formed. The reason is that the quantization of the energy levels in a nanomentric trap reduces considerably the number of accessible states. As a consequence, the spin–exchange processes are blocked. The necessity to use small pores for the detection of the di-positronium molecule, was discussed in ref. [23]. The authors considered a porous material containing a regular array of small interconnected pores (4 nm radius) that formed a series of cylinders with axes orthogonal to the external surface of the material. By using this geometry, the particles move freely along the axis of the cylinder. The appearance of a continuum of states (even in a single direction) enhances the spin quenching mechanisms, which become dominant over the formation of Ps_2 molecules.

Here we have considered large pores (radius $R = 100 - 300$ nm). In such a situation, the vast majority of the particle–particle interactions takes place inside the sphere. Indeed, since the range of the interaction potential with the surface is around $R_i \approx 0.2$ nm $\ll R$, the fraction of particles in contact with the pore surface is small compared to the total number of particles. Moreover, the simulations show that the gas is rapidly polarized. Once the system becomes fully polarized, the production of Ps_2 stops [27]. In summary, in our model we assume that the dominant Ps collision processes are the ^{3}Ps–^{3}Ps and ^{3}Ps–^{1}Ps scattering events and we discard the Ps quenching that is due to the formation of Ps_2 molecules.

We consider a gas of positronium obtained from a highly energetic beam of collimated positrons impinging on a porous silica sample. We assume that the Ps atoms are principally formed in proximity to interstitial defects or cavities. The value of the mean emission energy E_0 of the positronium atoms determines the initial state of the gas. Experimental findings, corroborated by the theoretical model developed by Nagashima *et al* [20], lead to the estimate $E_0 \simeq 0.6$ eV (or at least in the range between 0.5 and 3 eV). This value seems to be quite independent from the initial kinetic energy of the positron beam. Accordingly, we assume that the initial particle distribution f_i that describes the injection of the atoms in the material, is given by a shifted Maxwell–Boltzmann distribution

$$f_i = \frac{n_i}{n_c} e^{-\frac{1}{\Delta_E}\frac{(E-E_0)^2}{2m}}, \tag{4}$$

where

$$n_c \equiv \left(\frac{\Delta_E m}{2\pi\hbar^2}\right)^{3/2}$$

and n_i is the initial particle density of the ith population. In equation (4), Δ_E is the variance of the atomic energy distribution around the mean value E_0 (in our simulations we take $\Delta_E = 0.1$ eV). Equation (4) represents a highly out-of-equilibrium distribution of particles. The two-particle hard-sphere interactions cause a rapid redistribution of the energy among the particles. As a result, after few scattering events, the gas of positronium is well described by a Bose–Einstein distribution [37].

We now calculate the initial composition of the positronium gas. We consider a spin-polarized source of positrons. We denote by P the initial polarization of the positrons injected in the solid

$$P = \frac{p_\uparrow - p_\downarrow}{p_\uparrow + p_\downarrow} = q_+ - q_-\,, \tag{5}$$

where $p_\uparrow$, $p_\downarrow$ are, respectively, the number of positrons with spin up and spin down and $q_+ = \frac{p_\uparrow}{p_\uparrow + p_\downarrow} = \frac{1+P}{2}$ ($q_- = \frac{p_\downarrow}{p_\uparrow + p_\downarrow} = \frac{1-P}{2}$) denotes the fraction of spin-up (spin-down) positrons. The electrons in the target are unpolarized. Consequently, the positronium gas formed in the sample has the following composition:

$$\begin{aligned}
&\frac{q_+}{2}\left(\left|e^-\uparrow, e^+\uparrow\right\rangle + \left|e^-\downarrow, e^+\uparrow\right\rangle\right)\\
&+\frac{q_-}{2}\left(\left|e^-\uparrow, e^+\downarrow\right\rangle + \left|e^-\downarrow, e^+\downarrow\right\rangle\right)\\
&=\frac{q_+}{2}\,|1,1\rangle + \frac{q_+}{4}(|1,0\rangle + |0,0\rangle)\\
&+\frac{q_-}{4}(|1,0\rangle + |0,0\rangle) + \frac{q_-}{2}\,|1,-1\rangle\\
&=\frac{q_+}{2}\,|1,1\rangle + \frac{1}{4}(|1,0\rangle + |0,0\rangle)\\
&+\frac{q_-}{2}\,|1,-1\rangle=\\
&\underbrace{\frac{1+P}{4}\,|1,1\rangle + \frac{1}{4}\,|1,0\rangle + \frac{1-P}{4}\,|1,-1\rangle}_{^3\mathrm{Ps}}\\
&+\underbrace{\frac{1}{4}\,|0,0\rangle}_{^1\mathrm{Ps}},
\end{aligned} \tag{6}$$

where we used equations (1)–(2) and $q_+ + q_- = 1$. According to equation (6), the initial densities of the various populations are

$$\begin{aligned}
n_{11} &= \frac{1+P}{4} n_{ini}\\
n_{10} &= \frac{1}{4} n_{ini}\\
n_{1-1} &= \frac{1-P}{4} n_{ini}\\
n_{00} &= \frac{1}{4} n_{ini},
\end{aligned}$$

where n_{ini} denotes the total initial density of the positronium. The particle densities are obtained by taking the zeroth-order moment of the distribution function

$$n_i = \frac{1}{(2\pi\hbar)^3}\int f_i(\mathbf{p})\,\mathrm{d}\mathbf{p};\;\; i = (11), (10), (1-1), (00)\;. \tag{7}$$

We consider a uniform gas. From the numerical point of view, it is convenient to change the dynamical variable of equation (3) and to express the atomic distribution function in terms of the energy $E = \frac{|\mathbf{p}|^2}{2m}$. In order to give more details on the numerical discretization procedure that we adopted in our

code, let us consider the scattering kernel between two particles of the same kind (the other cases are treated in the same way)

$$\begin{aligned} Q[f](\mathbf{p}_1) \equiv g^2 \int \Big[& \big(1+f_1\big)\big(1+f_2\big) f_3 f_4 \\ & - f_1 f_2 \big(1+f_3\big)\big(1+f_4\big)\Big] \\ & \times \delta\big(E_1+E_2-E_3-E_4\big) \\ & \times \delta\big(\mathbf{p}_1+\mathbf{p}_2-\mathbf{p}_3-\mathbf{p}_4\big)\, \mathrm{d}\mathbf{p}_2\, \mathrm{d}\mathbf{p}_3\, \mathrm{d}\mathbf{p}_4\,, \end{aligned} \tag{8}$$

where $g^2 = c\sigma_{i,i\to i,i}$ is the scattering rate of the process, f is the atomic distribution function and we introduced the shorthand notations $f_i \equiv f(\mathbf{p}_i)$, $E_i \equiv E(\mathbf{p}_i)$. In our simulations we make the hypothesis that the distribution functions depend only by the modulus of the momentum $p \equiv |\mathbf{p}|$ and we denote $h(E) = f(\sqrt{2mE})$. Then, writing $\mathrm{d}\mathbf{p} = p^2\, \mathrm{d}p\, \mathrm{d}\hat{\mathbf{p}}$ where the hat denotes the unit vector, equation (8) becomes

$$\begin{aligned} Q[h](E_1) = g^2 \int \Big[& \big(1+h_1\big)\big(1+h_2\big) h_3 h_4 \\ & - h_1 h_2 \big(1+h_3\big)\big(1+h_4\big)\Big] p_2^2\, p_3^2\, p_4^2 \\ & \times \delta\big(E_1+E_2-E_3-E_4\big)\, \delta\big(\mathbf{p}_1+\mathbf{p}_2+\mathbf{p}_3+\mathbf{p}_4\big) \\ & \times \mathrm{d}p_2\, \mathrm{d}p_3\, \mathrm{d}p_4\, \mathrm{d}\hat{\mathbf{p}}_2\, \mathrm{d}\hat{\mathbf{p}}_3\, \mathrm{d}\hat{\mathbf{p}}_4\,, \end{aligned} \tag{9}$$

where we have set $h_i = h(E_i)$ and we have made the substitutions $\mathbf{p}_2 \to -\mathbf{p}_2$, $\mathbf{p}_3 \to -\mathbf{p}_3$. Next, we consider the angular integration in equation (9)

$$\begin{aligned} \mathcal{I} &= \int \delta\big(\mathbf{p}_1+\mathbf{p}_2+\mathbf{p}_3+\mathbf{p}_4\big)\, \mathrm{d}\hat{\mathbf{p}}_2\, \mathrm{d}\hat{\mathbf{p}}_3\, \mathrm{d}\hat{\mathbf{p}}_4 \\ &= \frac{1}{(2\pi)^3} \int e^{i(\mathbf{p}_1+\mathbf{p}_2+\mathbf{p}_3+\mathbf{p}_4)\cdot\eta} \eta^2\, \mathrm{d}\eta\, \mathrm{d}\hat{\eta}\, \mathrm{d}\hat{\mathbf{p}}_2\, \mathrm{d}\hat{\mathbf{p}}_3\, \mathrm{d}\hat{\mathbf{p}}_4. \end{aligned}$$

Using

$$\begin{aligned} \int e^{i\mathbf{p}\cdot\eta}\, \mathrm{d}\hat{\mathbf{p}} &= \int e^{i\mathbf{p}\cdot\eta}\, \mathrm{d}\hat{\eta} \\ &= 2\pi \int_0^\pi e^{ip\eta\cos\phi} \sin\phi\, \mathrm{d}\phi = 4\pi \frac{\sin p\eta}{p\eta}, \end{aligned} \tag{10}$$

where ϕ denotes the angle between $\mathbf{p}$ and η, we obtain

$$\mathcal{I} = \frac{32\pi}{p_1 p_2 p_3 p_4} \int_0^\infty \frac{\sin(p_1\eta)\sin(p_2\eta)\sin(p_3\eta)\sin(p_4\eta)}{\eta^2}\, \mathrm{d}\eta.$$

We write the sinus functions in terms of the exponentials and use the following formula of the Fourier transform in the distribution space

$$\lim_{\varepsilon\to 0^+} \left[\int_{-\infty}^{-\varepsilon} \frac{e^{ip\eta}}{\eta^2}\, \mathrm{d}\eta + \int_\varepsilon^\infty \frac{e^{ip\eta}}{\eta^2}\, \mathrm{d}\eta \right] = \frac{2}{\varepsilon} - \pi|p|. \tag{11}$$

We obtain

$$\begin{aligned} \mathcal{I} = \frac{2\pi^2}{p_1 p_2 p_3 p_4} \big(& \big|p_1 - p_2 + p_3 + p_4\big| + \big|p_1 - p_2 - p_3 - p_4\big| \\ & + \big|p_1 + p_2 + p_3 - p_4\big| + \big|p_1 + p_2 - p_3 + p_4\big| \\ & - \big|p_1 - p_2 + p_3 - p_4\big| - \big|p_1 - p_2 - p_3 + p_4\big| \\ & - \big|p_1 + p_2 - p_3 - p_4\big| - \big|p_1 + p_2 + p_3 + p_4\big| \big). \end{aligned}$$

After few manipulations we have (the details are given in appendix)

$$\begin{aligned} \mathcal{I} = \frac{2\pi^2}{p_1 p_2 p_3 p_4} \big(& - \max\big(|p_1 - p_3|, |p_2 - p_4|\big) \\ & - \max\big(|p_2 - p_3|, |p_1 - p_4|\big) \\ & + \min\big(p_1 + p_3, p_2 + p_4\big) \\ & + \min\big(p_2 + p_3, p_1 + p_4\big)\big). \end{aligned} \tag{12}$$

Equation (9) becomes

$$\begin{aligned} Q[h](E_1) = g^2 \frac{\sqrt{2}\pi^2 m^{5/2}}{\sqrt{E_1}} \int \Big[& \big(1+h_1\big)\big(1+h_2\big) h_3 h_4 \\ & - h_1 h_2 \big(1+h_3\big)\big(1+h_4\big)\Big] \\ & \big(- \max\big(|p_1 - p_3|, |p_2 - p_4|\big) \\ & - \max\big(|p_2 - p_3|, |p_1 - p_4|\big) \\ & + \min\big(p_1 + p_3, p_2 + p_4\big) \\ & + \min\big(p_2 + p_3, p_1 + p_4\big)\big) \\ & \times \delta\big(E_1 + E_2 - E_3 - E_4\big) \\ & \times \mathrm{d}E_2\, \mathrm{d}E_3\, \mathrm{d}E_4, \end{aligned} \tag{13}$$

where $p_i = \sqrt{2mE_i}$ and we used $p\, \mathrm{d}p = m\, \mathrm{d}E$. This expression can be simplified by interchanging the p_3 and p_4 variables in the integral. We obtain the final formula

$$\begin{aligned} Q[h](E_1) &= 2g^2 \frac{\sqrt{2}\pi^2 m^{5/2}}{\sqrt{E_1}} \int \Big[\big(1+h_1\big)\big(1+h_2\big) h_3 h_4 \\ &\quad - h_1 h_2 \big(1+h_3\big)\big(1+h_4\big)\Big] \\ &\quad \times \Big[\min\big(p_1 + p_3, p_2 + p_4\big) \\ &\quad - \max\big(|p_1 - p_3|, |p_2 - p_4|\big)\Big] \\ &\quad \times \delta\big(E_1 + E_2 - E_3 - E_4\big) \\ &\quad \times \mathrm{d}E_2\, \mathrm{d}E_3\, \mathrm{d}E_4 \\ &= g^2 \frac{4\pi^2 m^3}{\sqrt{E_1}} \int_0^\infty \mathrm{d}E_2 \int_0^{E_1+E_2} \\ &\quad \times \mathrm{d}E_3 \Big[\min\big(E^+, \tilde{E}^+\big) - \max\big(E^-, \tilde{E}^-\big)\Big] \\ &\quad \times \Big[\big(1+h_1\big)\big(1+h_2\big) h_3 h\big(E_1+E_2-E_3\big) \\ &\quad - h_1 h_2 \big(1+h_3\big)\big(1+h\big(E_1+E_2-E_3\big)\big)\Big], \end{aligned} \tag{14}$$

where

$$\begin{aligned} E^\pm &= \big|\sqrt{E_1} \pm \sqrt{E_3}\big| \\ \tilde{E}^\pm &= \big|\sqrt{E_2} \pm \sqrt{E_1+E_2-E_3}\big|. \end{aligned}$$

A similar expression for the numerical discretization of the boson scattering kernel has been obtained by Snoke with a different approach [38]. We have integrated numerically the Boltzmann scattering operator (14) by using a deterministic approach [39, 40]. We have used a uniform discretization

mesh for the energy variable. The time-dependent derivative of equation (3) is approximated by a third-order Runge–Kutta method with total-variation diminishing properties [41].

3. Numerical results

We simulate the evolution of the singlet and triplet components of the Ps gas for different gas densities. In particular, we compare the gas lifetime for the case of an unpolarized and a spin-polarized gas. First, we consider a gas of positronium without spin polarization ($P = 0$). In this case, all the positronium states have the same initial density ($n_i = n_{ini}/4$ for all i). We fix the total initial Ps density $n_{ini} = 10^{-5}$ nm^{-3}. The results of the calculations are shown in figure 1. The transformation of the ortho-positronium into para-positronium is quite efficient. The positronium is rapidly quenched by the two-body collision processes. The simulation shows that the ortho-positronium populations decay on a similar time scale (around 5-10 ns), while the para-positronium component decays faster (the decay time is around 200 ps). After 30 ns, which is about 5 times smaller than the free ortho-positronium lifetime, the density of the gas is almost zero.

Next, we compute the evolution of a partially spin-polarized gas, and we focus in particular on the time necessary to obtain a fully spin-polarized gas. We set the initial polarization $P = 30\%$. Our results can be compared with the experiments described in [27]. The authors observe the almost-complete spin polarization of the gas in a time shorter than 50 ns. In the left panel of figure 2, we depict the evolution of the gas populations (according to [27], we set the atomic density $n_{ini} = 5 \times 10^{-6}$ nm^{-3}). After 0.5 ns, the density of para-positronium is almost zero (inset in the left panel of figure 2). The triplet states decay with a time scale between 8 and 15 ns, and after around 20 ns, a single atomic population ($|1, 1\rangle$) is present. As it can be seen from equation (1), in the $|1, 1\rangle$ state the electron and the positron have the same spin direction. When two $|1, 1\rangle$ atoms collide, the conservation of the total angular momentum prevents the creation of the other Ps species. In this way, a fully spin-polarized system is no longer affected by the spin quenching effects. In the right panel of figure 2, we depict the polarization curve of the positronium gas. In agreement with the experimental results described in [27], our simulations show that the time necessary to reach the complete polarization of Ps is around 30 ns.

In figure 3 we display the evolution of a gas with higher density (initial positronium density equal to 7×10^{-4} nm^{-3}) and with the same positron polarization as in the previous case ($P = 30\%$). In the left panel, we depict the time evolution of the singlet and triplet states. Also in this case, the spin–exchange scattering reactions cause the quenching of the ortho-positronium until only the majority spin component remains in the gas. After around 1 ns, the density drops to 10^{-4} nm^{-3} and the gas is formed only of the triplet state $|1, 1\rangle$. In particular, the decay rate of the short-lived para-positronium state is nearly the same as what was found in the case depicted in figure 2. This trend is due to the different

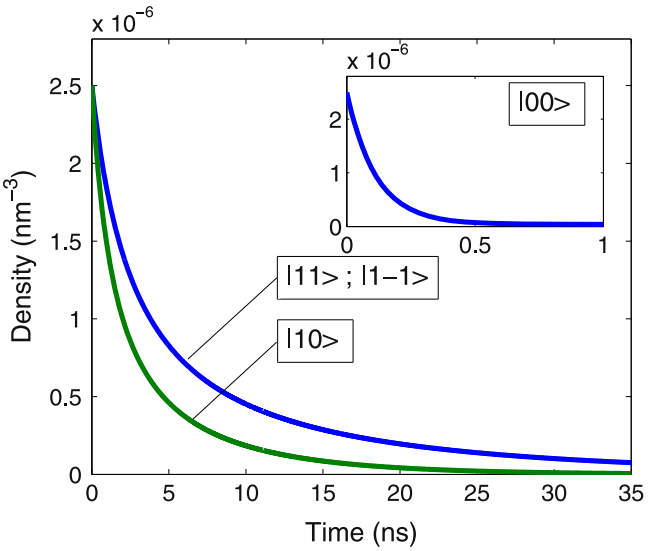

Figure 1. Quenching of Ps. Evolution of the density of the triplet $|1, 1\rangle, |1, -1\rangle$ (blue), and $|1, 0\rangle$ (green) populations. In the inset we depict the singlet state population.

production rate of para-positronium by the Ps–Ps collisions. Since the atomic collision rate increases with increasing density, when the density of the gas is large, the para-positronium is efficiently produced. This explains the fast decay of all the ortho-positronium populations during the first nanosecond ($n_{ini} = 7 \times 10^{-4}$ nm^{-3}).

The spin polarization P of the gas is depicted in the right panel of figure 3. By comparison with the simulation depicted in figure 2, we see that in this case, the polarization process is nearly 20 times faster.

We also investigated how the spin polarization time depends on the positronium density. In figure 4 we depict the time at which the gas reaches 95% of polarization. When the gas density increases, the probability that two atoms collide and thus the para-positronium is formed increases. The behavior of the polarization time can be interpreted in terms of the bi-atomic collision time τ_c. As a simple estimation for τ_c, we have $\tau_c = \frac{\lambda}{v}$, where $v = \sqrt{2\frac{E}{m}}$ is the mean particle velocity, $E$is the atomic energy, and λ is the mean free path between two consecutive Ps–Ps collisions. λ can be estimated by the following formula $\lambda = \frac{1}{\sqrt{2}\sigma n}$, where σ is the cross section of the dominant interaction channel and n the gas density [42].

In our simulation, we have included all the relevant scattering processes with atomic conversion (PAC) and without atomic conversion (PWC) that are described in table 1. Although the scattering rates related to the PWC are of the same order of magnitude as those of the PAC, the influence on the evolution of the gas of this two types of processes is very different. During the spin polarization process of the positronium gas, we observe two main dynamical mechanisms: (i) the atomic thermalization and (ii) the atomic conversion (the change of the total number of atoms of each Ps species). The thermalization mechanism is a relatively fast

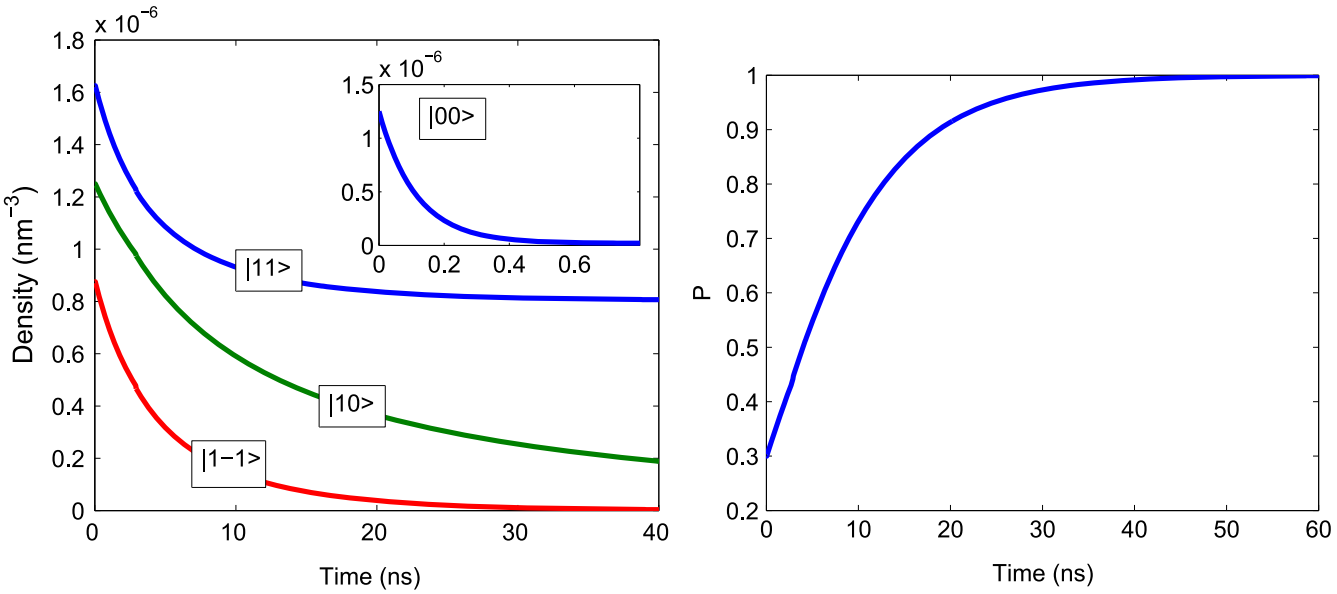

Figure 2. Left panel: quenching of Ps. Evolution of the triplet $|1, 1\rangle$ (blue), $|1, 0\rangle$ (green), $|1, -1\rangle$ (red) and singlet $|0, 0\rangle$ (inset) populations. Right panel: time evolution of the spin polarization P of the positronium gas.

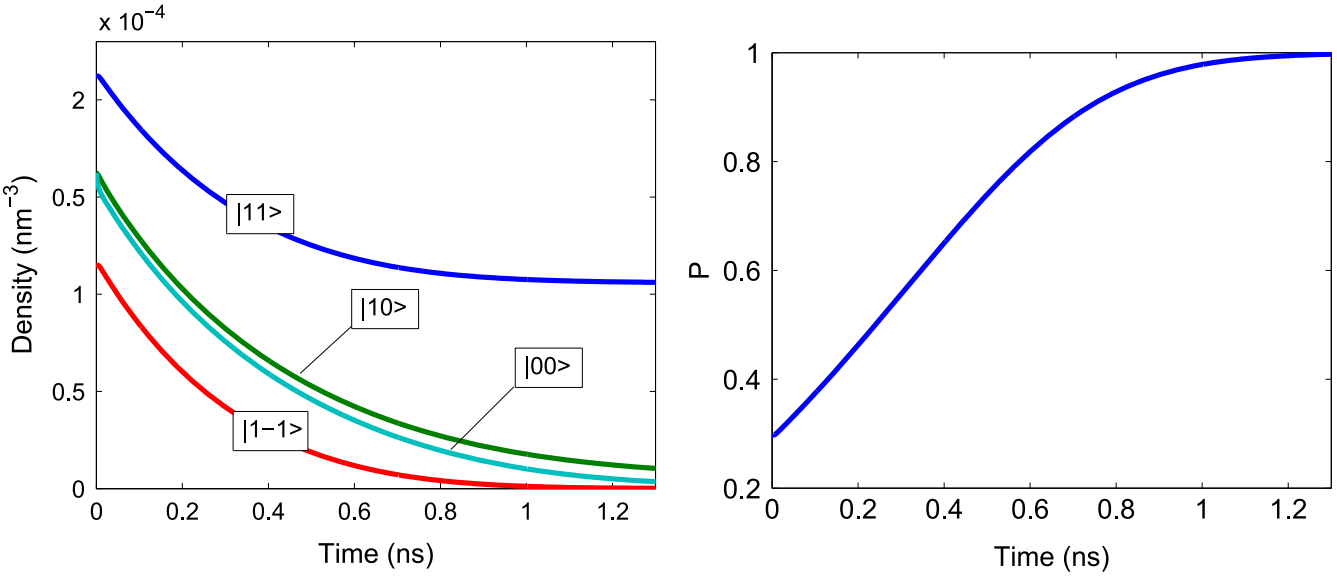

Figure 3. Left panel: Positronium quenching process. Evolution of the triplet $|1, 1\rangle$ (blue), $|1, 0\rangle$ (green), $|1, -1\rangle$ (red) and singlet $|0, 0\rangle$ (cyan) populations. Right panel: Time evolution of the spin polarization P.

process (for a Ps gas with density of 7×10^{-4} nm^{-3} it takes around 100 ps) during which the total energy of the gas is redistributed among the atoms. At the end of this stage, the atomic populations f_i are well described by a Bose–Einstein distribution with a certain temperature and chemical potential. When the gas reaches the thermal equilibrium, the collision processes without atomic conversion (PWC) cannot change the atomic distribution function. On the contrary, the PAC collisions may change the number of atoms of the various Ps populations. The PAC are thus responsible for the modification of the total number of atoms of the different Ps populations and are at the basis of the quenching mechanism. The PWC play a role only in the internal thermalization of the atoms. Since the thermalization is faster than the quenching mechanism, the PWC influence only the first part of the dynamical evolution of the gas and have little impact on the remaining spin polarization process.

We estimate the characteristic time of the Ps spin polarization by considering the rate at which the ortho-positronium is converted into para-positronium. Our numerical results indicate that the dominant scattering channels that lead to the spin polarization of the gas and to the annihilation of the ortho-Ps are $|1, 1\rangle + |1, -1\rangle \rightarrow |0, 0\rangle$ and $|1, 0\rangle + |1, 0\rangle \rightarrow |0, 0\rangle$. According to table 1, we see that

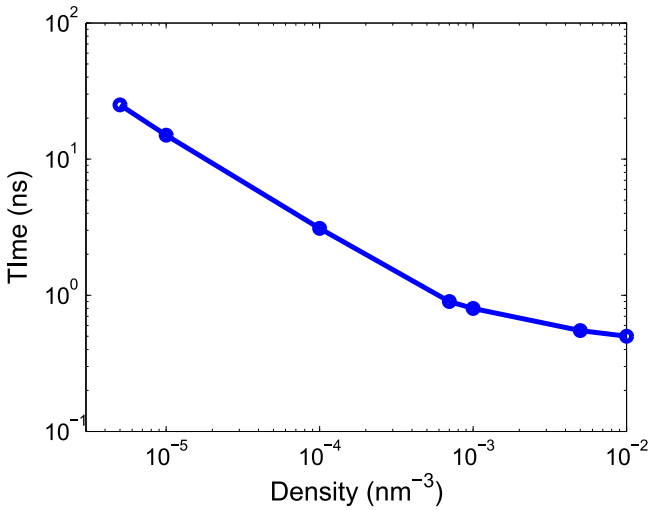

Figure 4. Time necessary to reach 95% of spin polarization as a function of the positronium density. The initial spin polarization $P = 30\%$.

the cross section for these processes is $\sigma \simeq 27\ \pi a_0^2$. We obtain

$$\tau_c = \frac{1}{2\sigma n}\sqrt{\frac{m}{E}} = \frac{20}{n}\ \text{fs}, \tag{15}$$

where the density in expressed in nm^{-3} and we set $E = 0.1$ eV. When the gas density is higher than 10^{-4} nm^{-3} the collision time is shorter than the p–Ps lifetime. In this regime, the p–Ps is efficiently produced and the polarization rate is limited by the annihilation rate of the p–Ps. On the contrary, when the gas density is lower than 10^{-4} nm^{-3}, the probability that two atoms collide, and thus that the p–Ps is formed, is smaller than the probability that the p–Ps annihilates. For this reason, the particle annihilations rate becomes proportional to the collision frequency τ_c^{-1}. This two-scale behavior is clearly displayed in figure 4.

4. Conclusion

In this paper, we analyzed the population dynamics of a positronium gas produced by implantation of high energy spin-polarized positrons in a porous solid. The atomic evolution was simulated by a kinetic Boltzmann equation and all the relevant two-body interactions were included in our calculations. In particular, we focused on the impact of the spin quenching mechanisms on the total lifetime of the gas. The theoretical study revealed that when the positronium density is sufficiently high and the gas is spin-polarized, the minority spin component of the gas is rapidly suppressed by annihilation with the same amount of atoms polarized in the opposite direction. As a result, the gas becomes fully polarized before the complete annihilation of the positronium. Furthermore, we showed that the decay rates of the ortho-positronium populations are sensitive to the value of the gas density. For a high-density gas, the decay rate of the o–Ps populations is close to the p–Ps decay time. In particular, for a density of the order of 10^{-3} nm^{-3}, this process (elimination of the minority component) requires around 1 ns. This time scale is rather short if compared with the ortho-positronium lifetime.

Acknowledgments

This work was partially funded by the Agence Nationale de la Recherche (contract ANR-10-BLAN-0420).

Appendix. Simplification of the scattering integral

In order to verify equation (12), we define

$$\begin{aligned} A \equiv & \left|p_1 - p_2 + p_3 + p_4\right| + \left|p_1 - p_2 - p_3 - p_4\right| \\ & + \left|p_1 + p_2 + p_3 - p_4\right| + \left|p_1 + p_2 - p_3 + p_4\right| \\ & - \left|p_1 - p_2 + p_3 - p_4\right| - \left|p_1 - p_2 - p_3 + p_4\right| \\ & - \left|p_1 + p_2 - p_3 - p_4\right| - \left(p_1 + p_2 + p_3 + p_4\right), \end{aligned}$$

and we show that

$$\begin{aligned} A = & \min\left(p_1 + p_3, p_2 + p_4\right) + \min\left(p_2 + p_3, p_1 + p_4\right) \\ & - \max\left(\left|p_1 - p_3\right|, \left|p_2 - p_4\right|\right) \\ & - \max\left(\left|p_2 - p_3\right|, \left|p_1 - p_4\right|\right). \end{aligned} \tag{A.1}$$

From the conservation of the total momentum expressed by the delta distribution in equation (9), the integral is restricted to the manifold $\mathbf{p}_1 + \mathbf{p}_2 + \mathbf{p}_3 + \mathbf{p}_4 = 0$. Consequently, the following inequality holds true for the modulus $p_i \leqslant S - p_i$ where $i = 1, \ldots, 4$ and $S = \sum_i p_i$. We have

$$\begin{aligned} & \left|p_1 - p_2 + p_3 + p_4\right| + \left| - p_1 + p_2 + p_3 + p_4\right| \\ & \quad + \left|p_1 + p_2 + p_3 - p_4\right| + \left|p_1 + p_2 - p_3 + p_4\right| \\ & \quad = \left|S - 2p_1\right| + \left|S - 2p_2\right| + \left|S - 2p_3\right| + \left|S - 2p_4\right| = 2S, \end{aligned}$$

where in the last equality we used $2p_i \leqslant S$ for $i = 1, \ldots, 4$. We obtain

$$\begin{aligned} A = & -\left|p_1 - p_2 + p_3 - p_4\right| - \left|p_1 - p_2 - p_3 + p_4\right| \\ & - \left|p_1 + p_2 - p_3 - p_4\right| + \left(p_1 + p_2 + p_3 + p_4\right) \end{aligned}$$

By using the following identities (a, b, c, d are real numbers)

$$\begin{aligned} & 2\max\left(|a|, |b|\right) = |a + b| + |a - b| \\ & 2\min\left(c, d\right) = c + d - |c - d| \quad c, d > 0 \end{aligned}$$

we obtain

$$\begin{aligned} & 2\min\left(p_1 + p_3, p_2 + p_4\right) + 2\min\left(p_2 + p_3, p_1 + p_4\right) \\ & \quad = 2\left(p_1 + p_3 + p_2 + p_4\right) - \left|p_1 + p_3 - p_2 - p_4\right| \\ & \quad - \left|p_2 + p_3 - p_1 - p_4\right| \end{aligned} \tag{A.2}$$

$$
\begin{aligned}
&2\max\left(\left|p_1-p_3\right|,\left|p_2-p_4\right|\right)\\
&\quad+2\max\left(\left|p_2-p_3\right|,\left|p_1-p_4\right|\right)\\
&\quad=\left|p_1-p_3+p_2-p_4\right|+\left|p_1-p_3-p_2+p_4\right|\\
&\quad+\left|p_2-p_3+p_1-p_4\right|+\left|p_2-p_3-p_1+p_4\right|. \qquad \text{(A.3)}
\end{aligned}
$$

The sum of equation (A.2) and equation (A.3) provides equation (A.1).

References

[1] Karplus R and Klein A 1952 *Phys. Rev.* **87** 848
[2] Mills A P 2002 *Nucl. Instrum. Methods Phys. Res. Sect.* B **192** 415
[3] Platzman P M and Mills A P 1994 *Phys. Rev.* B **49** 454
[4] Debu P *et al* 2012 *Hyperfine Interact* **212** 51
[5] Perez P and Rosowsky A 2005 *Nucl. Instrum. Methods Phys. Res. Sect.* A **545** 20
[6] Amoretti M *et al* 2002 *Nature* **419** 456
[7] Gabrielse G *et al* 2004 *Phys. Rev. Lett.* **93** 073401
[8] Storry C H *et al* 2004 *Phys. Rev. Lett.* **93** 263401
[9] Cassidy D B, Hisakado T H, Tom H W K and Mills A P 2012 *Phys. Rev. Lett.* **108** 043401
[10] Gidley D W *et al* 2001 *New Directions in Antimatter Chemistry and Physics* ed C M Surko and F A Gianturco (Dordrecht: Kluwer Academic)
[11] Gidley D W, Frieze W E, Dull T L, Yee A F, Ryan E T and Ho H-M 1999 *Phys. Rev.* B **60** R5157
[12] Larrimore L, McFarland P N, Sterne P A and Bug A L R 2000 *J. Chem. Phys.* **113** 10642
[13] Brandt W and Paulin R 1968 *Phys. Rev. Lett.* **21** 193
[14] Perkal M B and Walters W A 1970 *J. Chem. Phys.* **53** 190
[15] Chuang S Y and Tao S J 1971 *J. Chem. Phys.* **54** 4902
[16] Takada S, Iwata T, Kawashima K, Saito H, Nagashima Y and Hyodo T 2000 *Radiat. Phys. Chem. (UK)* **58** 781
[17] Chang T, Xu M and Zeng X 1987 *Phys. Lett.* A **126** 189
[18] Kiefl R F and Harshman D R 1983 *Phys. Lett.* A **98** 447
[19] Mariazzi S, Bettotti P and Brusa R S 2010 *Phys. Rev. Lett.* **104** 243401
[20] Nagashima Y *et al* 1995 *Phys. Rev.* A **52** 258
[21] Petkov M P *et al* 2003 *J. Phys. Chem.* B **107** 2725
[22] Cassidy D B and Mills A P 2007 *Nature* **449** 195
[23] Cassidy D B and Mills A P 2008 *Phys. Rev. Lett.* **100** 013401
[24] Cassidy D B, Deng S H M, Greaves R G, Maruo T, Nishiyama N, Snyder J B, Tanaka H K M and Mills A P 2005 *Phys. Rev. Lett.* **95** 195006
[25] Liszkay L, Corbel C, Raboin L, Boilot J-P, Perez P, Brunet-Bruneau A, Crivelli P, Gendotti U, Rubbia A and Ohdaira T 2009 *Appl. Phys. Lett.* **95** 124103
[26] Brinker C J and Scherer G W 1990 *The Physics and Chemistry of Sol-Gel Processing* (New York: Academic Press)
[27] Cassidy D B, Meligne V E and Mills A P 2010 *Phys. Rev. Lett.* **104** 173401
[28] Banyai L, Gartner P, Schmitt O M and Haug H 2000 *Phys. Rev.* B **61** 8823
[29] Tassone F and Yamamoto Y 1999 *Phys. Rev.* B **59** 10830
[30] Gardiner C W, Lee M D, Ballagh R J, Davis M J and Zoller P 1998 *Phys. Rev. Lett.* **81** 5266
[31] Chakraborty S, Basu A and Ghosh A S 2004 *Nucl. Instrum. Methods* B **221** 112
[32] Ivanov I A, Mitroy J and Varga K 2001 *Phys. Rev. Lett.* **87** 063201
[33] Shumway J and Ceperley D M 2001 *Phys. Rev.* B **63** 165201
[34] Chakraborty S and Ghosh A S 2005 *Phys. Rev.* A **72** 052508
[35] Saito H and Hyodo T 2001 *New Directions in Antimatter Chemistry and Physics* ed C M Surko and F Gianturco (New York: Kluwer Academic) p 101
[36] Ivanov I A, Mitroy J and Varga K 2002 *Phys. Rev.* A **65** 022704
[37] Morandi O, Hervieux P-A and Manfredi G 2014 *Eur. Phys. J.* D **68** 176
[38] Snoke D W and Wolfe J P 1989 Population dynamics of a bose gas near saturation *Phys. Rev.* B **39** 4030–7
[39] Morandi O, Hervieux P-A and Manfredi G 2013 *Phys. Rev.* A **88** 23618
[40] Lichtenberger P, Morandi O and Schüerrer F 2012 *Phys. Rev.* B **84** 045406
[41] Shu C-W and Osher S 1988 *J. Comput. Phys.* **77** 439
[42] Chapman S and Cowling T G 1991 *The Mathematical Theory of Non-Uniform Gases* (New York: Cambridge University Press)